Asian Journal of Chemistry; Vol. 36, No. 9 (2024), 2063-2069

ASIAN JOURNAL OF CHEMISTRY

https://doi.org/10.14233/ajchem.2024.31105

Extraction of Nanocellulose Fiber from Agrowastes for Efficient Fluoride Removal: A Sustainable Approach

G. GATAWA[1], J. NAHURIRA[1], L. GAMANIEL[1], V. MAYANI[2], R. THAKER[1] and S. MAYANI[1,*]

[1]Department of Chemistry, Marwadi University, Rajkot-Morbi Road, P.O. Gauridad, Rajkot-360003, India
[2]Hansgold Chem Discovery Center, Hansgold Chemdiscoveries Pvt. Ltd., Rajkot-360006, India

*Corresponding author: E-mail: suranjana.mayani@marwadieducation.edu.in

Received: 24 December 2023; *Accepted*: 7 July 2024; *Published online*: 30 August 2024; AJC-21731

The subject of water defluorination is becoming increasingly important, owing to chronic diseases such as fluorosis, neurological impairment and bone softening caused by fluoride contamination of drinking water in excess of 1.5 mg L^{-1}. Agrowastes (cotton seed and groundnut shells), the commonly available and renewable resource, were used as the precursor for the production of nanocellulose fiber *i.e.* cotton seed nanocellulose fiber (CNF) and groundnut shell nanocellulose fiber (GNF) as an exceptional method for fluoride removal. The physico-chemical characterization techniques were employed to analyze the structure and morphology of the synthesized nanocellulose fibre. To optimize the adsorption process, the impacts of several parameters including pH, contact time and adsorbent dosage were evaluated. The maximum amount of fluoride that could be removed under ideal conditions was investigated using a UV-visible spectrophotometry and was found to be 90%. This approach offers several advantages such as low-cost raw materials, eco-friendly synthesis methods and a high-performance adsorbent.

Keywords: Nanocellulose, Agrowastes, Cotton seed shell, Groundnut shell, Adsorbents.

INTRODUCTION

Cellulose is a strong, insoluble fiber that plays a crucial role in maintaining the structural integrity of plant cell walls [1-4]. Cellulosic fibres can break down into nanocellulose, which varies in length and diameter depending on the structure. Due to the large surface area to bulk ratio of these materials, their properties differ from those of their corresponding bulk materials, allowing for the selective manipulation necessary to produce new products [5]. Among the numerous cellulose-based wastes generated in every community, agricultural waste often goes unnoticed. Food, animal and crop wastes are all included in agricultural waste, commonly referred to as agro-waste [6,7].

Recent studies have focused on exploring ways to utilize the lignocellulosic matter obtained from agricultural waste, which typically consists of cellulose, hemicelluloses, and lignin [8,9]. Since cellulose is composed of assemblies of D-glucose and, more interestingly, long molecular chains are formed through the covalent bonding of carbohydrates. This unusual polymer has drawn the interest of many researchers based on a number of reviews [10,11].

Nanocellulose is a material with great inherent qualities, including high mechanical strength, biocompatibility and transparency [12]. It also blends nanotechnology with sustainable and ecologically friendly techniques [13-15]. Cotton and wood are the primary sources for cellulose extraction, but it may also come from a wide range of other materials, including marine biomass, marine tunicate animals, invertebrates, bacteria, fungus, annual plants and various agro-industrial wastes [14-16]. Due to the potential to develop cellulose nanostructures with unique features not seen in bulk materials, cellulose has undoubtedly garnered more and more interest in recent decades. Cellulose nanocrystals (CNC) can be produced in two morphological shapes, rod-like or needle-like shape, having a compact and ordered cellulose structure, which gives it unique properties [17]. In general, the dimensions of CNC depend on the origin of cellulose and hydrolysis conditions [18,19].

Additionally, the nanocelluloses incorporate remarkable nanoscale material properties with vital cellulose capabilities

[20-26] enhancing recycling efforts and other nanotechnology applications. It is evident that interest in nanocellulose for water treatment is also growing quickly. However, to realize the full potential of nanocellulose for fabrication of water filtration membranes, it is essention to understand the process, structure and property relationship for nanocellulose membranes [27] for the water defluorination which has become increasingly important issue.

In present work, nanocellulose fiber (NCF) was synthesized from the agricultural wastes (cotton seed cover and groundnut seed shell) to remove fluoride from water in order to develop a cost-effective and sustainable method for the water treatment. The materials were characterized with scanning electron microscopy energy dispersive X-ray (SEM-EDX) transmission electron microscopy (TEM), X-ray diffraction (XRD), X-ray photoelectron spectroscopy (XPS) and thermogravimetric analysis (TGA) techniques. The maximum removal percentage of fluoride was achieved under optimized conditions and valilated with the UV-visible analysis, which confirmed that nanocellulose fiber can be used as an efficient, thermally stable recyclable and environmentally acceptable nanoadsorbent for the efficient removal of fluoride ions from the contaminated water.

EXPERIMENTAL

The chemicals *viz.* sodium hydroxide (Loba Chemie Pvt. Ltd., India; 97%), sulphuric acid (Loba Chemie Pvt. Ltd., India; 98%), hydrogen peroxide solution (Loba Chemie Pvt. Ltd., India; 30%), SPADNS (Chemdyes corporation, India), zirconyl chloride octahydrate (Chemdyes corporation, India, 98%), HCl (Molychem, India), sodium fluoride (Chemdyes corporation, India, 98.5 %) were procured and used without further purification. All the stock solutions were prepared in double distilled water.

Synthesis of nanocellulose fiber (NCF): Nanocellulose fiber (NCF) was prepared from two different agrowaste materials cotton seed and ground nut shells. The cotton seed and ground nut shells were washed, dried and crushed into the powder form. The powder of each starting material was treated with 2% NaOH for 3 h at 323 K on a magnetic stirrer to remove amorphous materials. This process was carried out three times to improve the crystal structure. The resultant solution was filtered and the residue washed with distilled water to neutralize the pH. The residue was bleached with 3% H_2O_2 and 4% NaOH at 50 ºC for 3 h on a magnetic stirrer. This procedure was further continued until the colour of powder become white. The residue was neutralized with distilled water and the acid treatment was done using 52% (w/w) sulphuric acid for 2 h at 318 K. To adhere the hydrolysis process, the solution was placed in cold water for 10 min. The solution was sonicated and after filtered and neutralized with distilled water. The residue was left to dry and then crushed in a mortar and pestle to make finer particles.

Removal of fluoride by nanocellulose composite: Fluoride removal studies were performed using the SPADNS method [28]. A solution containing fluoride was prepared by dissolving 110.5 mg anhydrous NaF in 500 mL distilled water. The working standard of fluoride solution was prepared by diluting 50 mL of stock standard up to 500 mL with distilled water. From the working standard, 50 mL was obtained and 100 mL of distilled water was added. To this solution, 1 mL of SPADNS reagent and 1 mL of zirconyl acid were added. The spectrophotometer (UV-1800, Shimadzu corporation, Japan) was used to examine the amount of fluoride present in the solution at 570 nm. In order to achieve equilibrium for the adsorption experiment, 0.5 g of adsorbent was added to this same solution and the mixture was placed on a rotary shaker (BioTechnics, India) for 30 min. The resultant solution was filtered using Whatman filter paper, and then analyzed the maximum absorption peak at 570 nm by using UV-visible spectrophotometer. The defluoridation studies were conducted at different experimental conditions like reaction time, amount of adsorbent, pH and temperature. The pH was adjusted to the desired level either with 0.1 M NaOH or 0.1 M HCl. The recyclability and reusability of the adsorbent were also tested by repeatedly washing with double distilled water and drying in air.

The fluoride removal efficiency in percentage was calculated according to the following relation:

$$\text{Fluoride removal } (\%) = \frac{C_o - C_t}{C_o} \times 100$$

where C_o and C_t are the initial concentration and the concentration (mol L^{-1}) at time t (min).

Characterization: Powder XRD measurements were performed on a laboratory X-ray diffractometer (30 mA, 40 kV; PANalytical Empyrean model DY1251 with PIXcel3D scanning line detector) using Cu*K*α radiation (λ =1.5406 Å) with a step size of 0.02626º and scan speed of 0.05252º/s in the 2θ range of 10 to 80º. The thermal analysis was carried out with TGA, SDT600, TA instrument, USA in the temperature range of 303-1073 K at the heating rate of 10 ºC min^{-1} in air atmosphere with a flow rate of 60 cm^3 min^{-1} using platinum crucibles. The surface morphology, elemental identification and quantitative compositional information of the material were determined with SEM-EDX, LEO-1430, VP, UK and TEM, JEM 2011, Jeol Corporation, Japan instruments.

RESULTS AND DISCUSSION

X-ray diffraction (XRD) pattern: The XRD spectra of the nanocellulose fiber derived from the cotton and groundnut shells are shown in Fig. 1. Three peaks appeared at 16.1º, 22.4º and 34.5º are attributed to (110), (200) and (004) planes in both adsorbents and thereby confirmed the presence of cellulose. After the chemical treatment, the adsorbents exhibit an increase in proportional crystallinity [29]. The amorphous nature of the cellulose structure is eliminated, which lead to an increase in the crystallinity index followed by the hydrolysis of lignin and hemicellulose found in cotton residues [30]. Additionally, the formation of cellulose nanocrystals, which can improve the crystallinity of the cellulose, may occur concurrently with the growth and realignment of monocrystals [31]. The increased crystallinity of the cellulose fibers was thought to enhance their stiffness, rigidity and strength. Consequently, the processed fibers had a higher possibility of exhibiting enhanced mechanical properties and reinforcing [32].

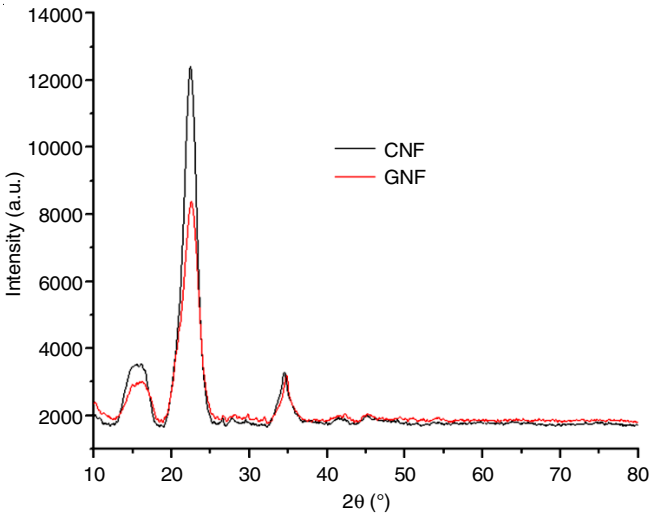

Fig. 1. X-ray diffraction of cotton seed nanocellulose fiber (CNF) and groundnut shell nanocellulose fiber (GNF) at wide-angle diffractions

SEM-EDX studies: The SEM images of cotton nanocellulose fiber (CNF, Fig. 2a) and groundnut nanocellulose fiber (GNF, Fig. 3a) had a rough surface, which is due to the degradation of hemicellulose and degradation of lignin by the repeated alkali treatment [33]. The morphological characteristics of the synthesized nanocellulose depicted in SEM micrographs at different magnifications shows the average diameter of 100 nm. The size of the nanocellulose was consistent with the reported values regarding the size of the nanocellulose [12,34]. The EDX spectrum of nanocellulose fibers (CNF and GNF) can be observed in Figs. 2b and 3b. It was found that each element has a unique atomic structure indicating a distinctive set of peaks for carbon, oxygen and sulphur for nanocellulose with respect to each of their binding energies.

TEM studies: In the TEM micrograph (Fig. 4), nanosized nanocellulose fibres of cotton and groundnut shells were clearly visible with nanorod-shaped fibres. According to TEM results, the size for nanocellulose's nanorods was 20 nm wide and less than 50 nm long.

XPS studies: By using XPS analysis, the variations in the nanocellulose fibers were quantitatively assessed. The predominant atomic compositions, C and O, of the both adsorbents confirmed the substantial cellulose contents (Tables 1 and 2).

TABLE-1
ELEMENTAL COMPOSITION OF COTTON SEED NANOCELLULOSE FIBER (CNF) BY X-RAY PHOTOELECTRON

Name	Atomic (%)	Peak BE	PP At. (%)
O1s	27.48	532.06	34.43
C1s	71.97	284.76	64.98
S2p	0.54	168.35	0.59

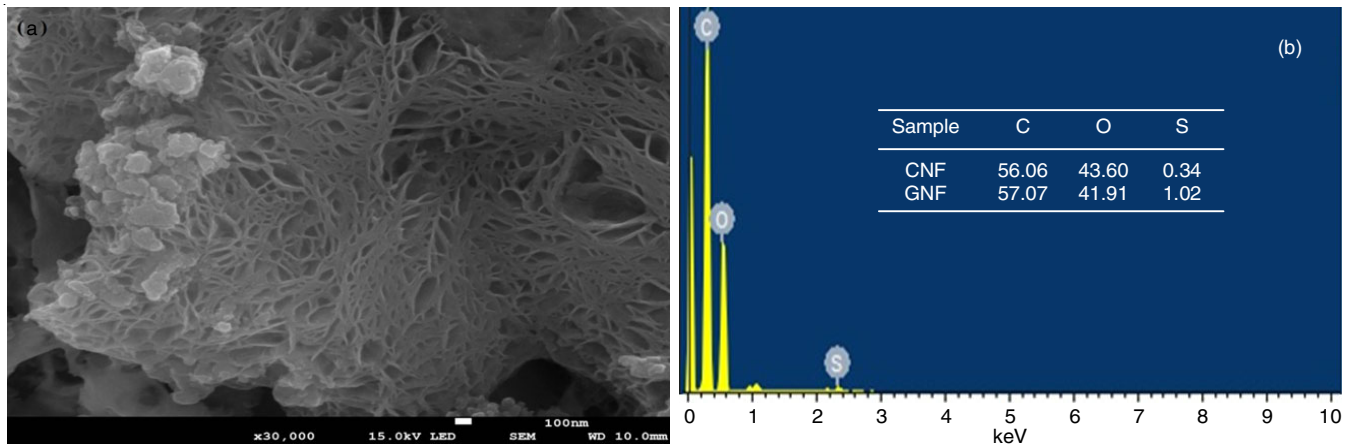

Fig. 2. SEM micrograph and EDX spectra of cotton seed shell nanocellulose fiber (CNF)

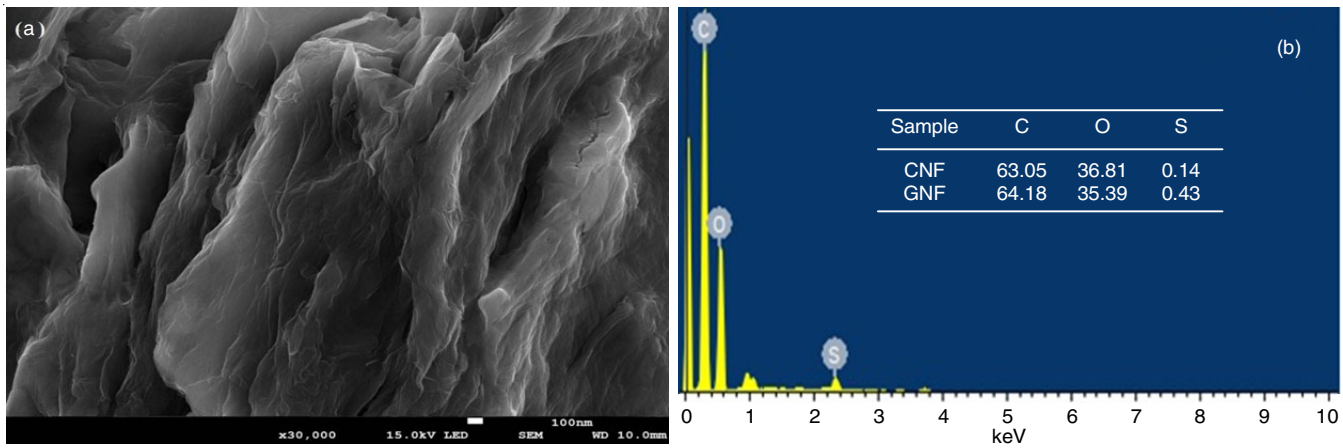

Fig. 3. SEM micrograph and EDX spectra of groundnut shell nanocellulose fiber (GNF)

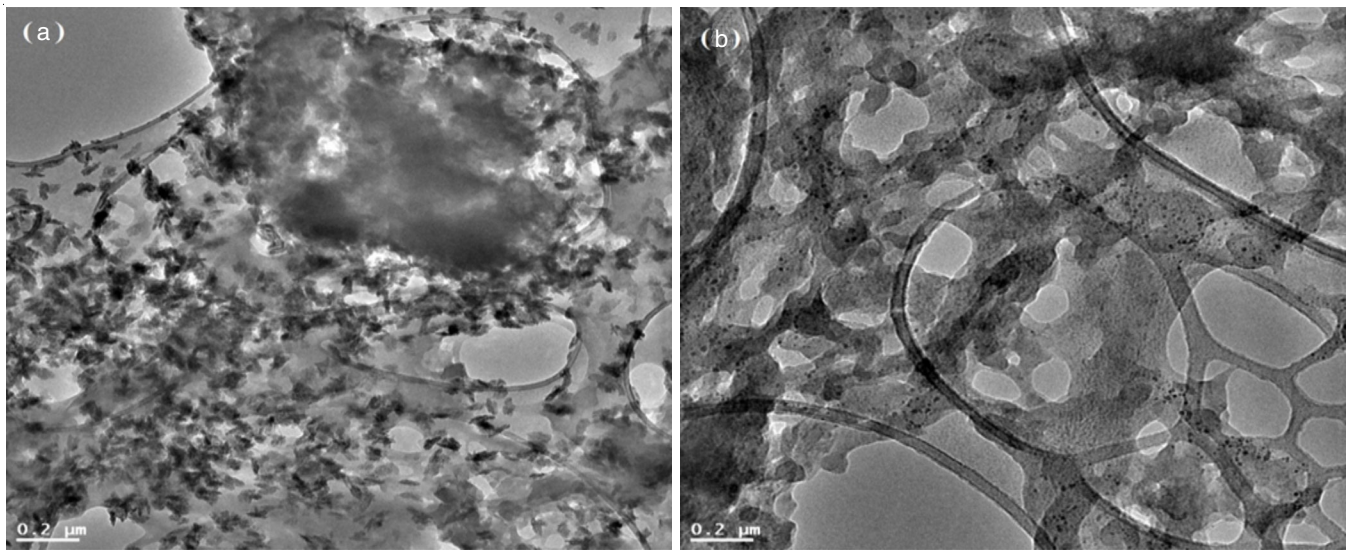

Fig. 4. TEM images of nanocellulose fiber obtained from cotton seed (a) and groundnut (b) shells

TABLE-2
ELEMENTAL COMPOSITION OF GROUNDNUT SHELL NANOCELLULOSE FIBER (GNF) BY X-RAY PHOTOELECTRON

Name	Atomic (%)	Peak BE	PP At. (%)
O1s	33.1	531.98	39.6
C1s	61.98	284.75	55.33
S2p	2.06	168.71	2.22
Si2p	2.15	102.22	2.37
N1s	0.71	400.26	0.48

Thermal studies: The thermal experiments were conducted in a N_2 atmosphere at temperatures ranging from 10 to 800 ºC. The loss of weight in nanocellulose fiber is due to cellulose degradation, which may include dehydration, depolymerization of hemicellulose, disintegration of α-1,4 glycoside linkages and rupture of hydroxyl groups [35]. All TGA curves had a tiny initial peak in the region of 10-140 ºC that was mostly caused by free and bound water evaporation, which resulted in weight losses (Fig. 5). At this stage, the nanocellulose from cotton seed shell experienced weight loss of 7% and 10% for that of groundnut shell. Due to the dehydration of cellulose fibres during acid hydrolysis, which led to the introduction of sulphate groups at the outer surface of nanocellulose, the moisture content of nanocellulose was lower than that of crude fibres [36-38]. The second-stage degradation of these materials took place at 140-300 ºC and 120-260 ºC for nanocellulose from cotton seed and groundnut shells, respectively. This deterioration weakens the adsorbents' capacity to crystallize and polymerize as well as the thermal stability during acid hydrolysis. At this stage, the nanocellulose from cotton experienced weight loss of 35% and 21% for that of groundnut. In the third stage degradation, the nanocellulose fibres from cotton and groundnut took place at 300-400 ºC and 260-360 ºC, respectively and experienced weight loss of 21% and 20%. The thermal stability of nanocellulose fibers are less as compared to pure cellulose TGA curves, which is due to the introduction of sulphate groups into the surface of the fiber during the sulfuric acid hydrolysis process. Sulphate groups have been suggested to hasten the dehydration of fiber [39]. Upon cleaning the raw materials, the hemicellulose and lignin undergo degradation, hence enhancing the thermal stability. These transitions were primarily related to the degradation of the cellulosic chain [40]. The maximum degradation of the nanocellulose fiber occurred at 400 ºC, exhibiting that nanocellulose fiber from cotton is somewhat more thermally stable than nanocellulose fiber from groundnut in which the maximum degradation occurred at 360 ºC. At this stage, they both experienced weight losses of 96%. The highest breakdown rates for nanocellulose fibres from cotton seed and groundnut shells occurred at 400-800 ºC and 360-800 ºC, respectively. This main degradation indicates complete pyrolysis of cellulose [41].

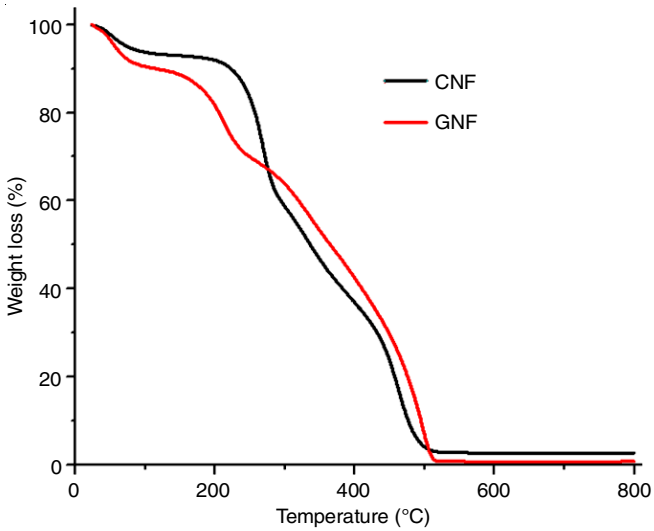

Fig. 5. Thermograms of nanocellulose fibre obtained from cotton seed and groundnut shells

Removal of fluoride using nanocellulose fiber: Enormous number of hydroxyl groups is found on the surface of nanocellulose fibre. These hydroxyl groups enable diverse chemical modifications on its surface. Nanocellulose fiber is an excellent, sustainable material that can be synthesized for

removing specific contaminants from water including fluoride. [42-44]. The adsorbents were subjected to several experimental conditions in order to determine its defluoridation ability. These conditions include the contact time, adsorbent load effect, pH of the solution and temperature effect.

Effect of contact time: The fluoride removal efficiency was investigated at different time at 30, 60, 90 and 180 min. By using CNF, the removal efficiency was 75, 80, 84 and 89%, respectively as compared to 79, 84, 88 and 90%, respectively for the GNF. Observing the efficiency of the adsorbent at different contact times while agitating the mixture on an orbital shaker, it was revealed that the adsorbent demonstrated high efficiency for the removal of fluoride as the contact time increased (Fig. 6). This shows that the removal % are high and almost have similar efficiencies.

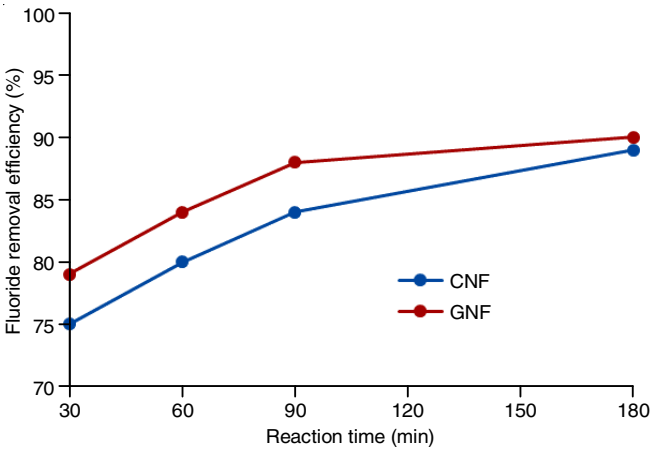

Fig. 6. Effect of contact time on the efficiency of removal of fluoride from water using CNF and GNF

The removal efficiency of fluoride was further carried out with UV visible spectrophotometer. The results show that with the increase of time the removal efficiency of fluoride was increased from 30 min to 180 min. The experiment has been carried out with nanocellulose Fibre using 0.5 g of adsorbent. The resultant solution was filtered using Whatman filter paper, and then analyzed the maximum absorption peak at 570 nm (Fig. 7). The high surface area and porosity of nanocellulose increase the contact between the fibers and fluoride ions, enhancing removal efficiency.

According to a study by Singh *et al.* [45], while percentage elimination originally increased as contact duration increased, over time it steadily decreased and eventually approximated a more or less constant number, signifying the achievement of equilibrium. The solute concentration gradient was strong and all of the adsorbent sites were initially empty, which may have contributed to these fluctuations in the rate of removal. The rate of fluoride uptake by the adsorbent dramatically decreased after that due to a reduction in adsorption sites. A decreased removal rate, especially near the end of the experiment, suggests that fluoride ions may formed a monolayer on the outer surface, as well as that pores on both adsorbents and pore diffusion onto the inner surface of adsorbent particles through the film, as a result of the constant shaking.

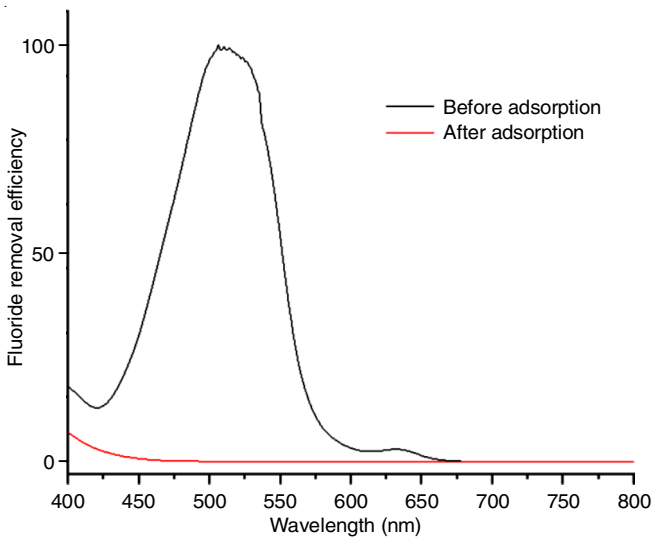

Fig. 7. UV-visible spectra for removal of fluoride before and after the adsorption

Effect of adsorbent load: The fluoride removal efficiency of adsorbent was investigated at different loads. At 2, 4 and 5 g/L, the removal efficiency was 64, 80 and 88%, respectively by using CNF and 67, 84 and 91%, respectively for GNF. The adsorbent showed a steady increase in fluoride removal efficiency as adsorbent load increased (Fig. 8). There is no discernible change in the percentage elimination of fluoride following a dose of 5 g/L. This shows that equilibrium is established at this dosage, which is caused by the active sites overlapping at larger dosages, decreasing the net surface area [46].

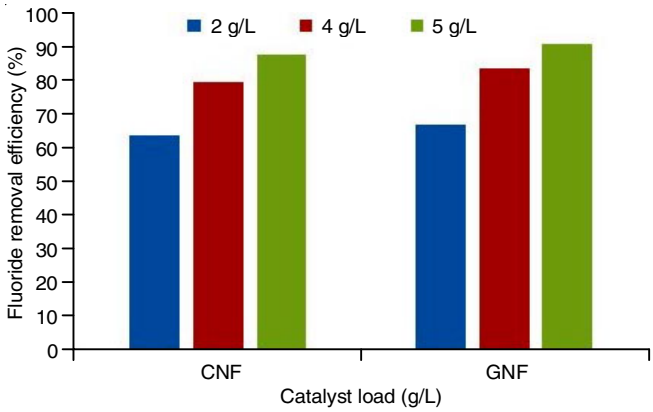

Fig. 8. Effect of catalyst load on the efficiency of removal of fluoride from water using CNF and GNF

Effect of the pH: The fluoride removal efficiency was also investigated at different pHs of solution. At pH 1, 5 and 9, the removal efficiency was 88, 79 and 64%, respectively by using CNF and 90, 82 and 66%, respectively for GNF (Fig. 9). From the results obtained, the fluoride removal efficiency showed a steady increase as the pH of the solution decreases as shown in Fig. 9. Both synthesized nanocellulose fibres exhibited high rates of adsorption for fluoride up to 90% of fluoride removal from water can be achieved.

Effect of temperature: The effect of temperature on the fluoride removal efficiency of the nanocellulose fibers was

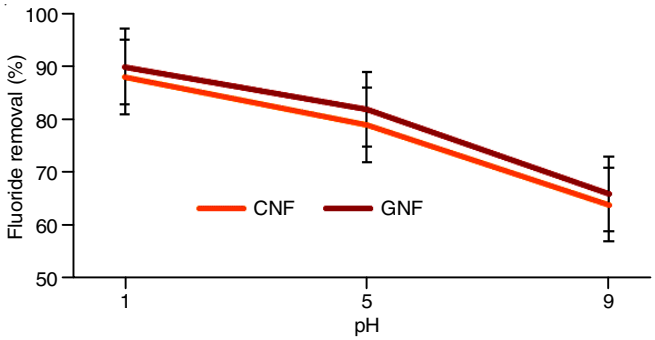

Fig. 9. Effect of pH of solution on the efficiency of removal of fluoride from water using CNF and GNF

observed at varying temperatures of 303, 323, 353 and 373 K. The removal efficiency was 85, 87, 89 and 90 %, respectively by using nanocellulose fiber from the cotton and 86, 88, 90 and 90%, respectively for nanocellulose fiber from groundnut. The efficiency of the adsorbent was moderate at 353 K in Fig. 10.

Reusability of NCF: After the first run of the catalytic removal of fluoride, the reaction mixture was filtered to obtain the used adsorbent. The adsorbent was thoroughly washed several times with distilled water and the residue, nanocellulose fiber was allowed to dry. The recovered adsorbent was again used directly in another run of the catalytic reaction till five cycles. It was found that five runs of the reaction could be carried out using the same adsorbent without any significant loss of performance in both cases (Fig. 11).

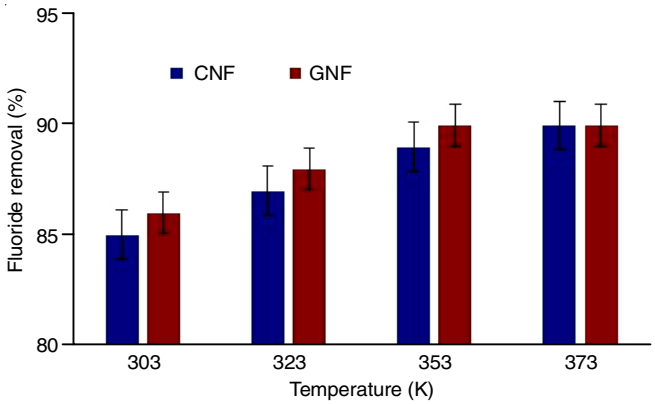

Fig. 10. Effect of temperature on the efficiency of removal of fluoride from water using CNF and GNF

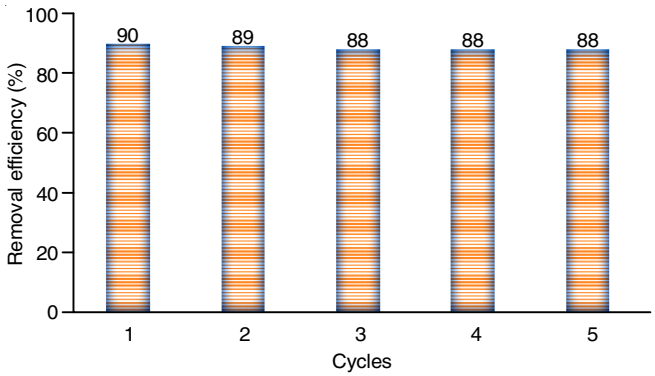

Fig. 11. Reusability capacity of nanocellulose fibre obtained from cotton seed and groundnut shells after 5 cycles

Conclusion

Before the successful extraction of cellulose from agricultural waste, pretreatment is a necessary step to remove lignin and hemicellulose. We have successfully prepared two different nanocellulose fibers from locally available agrowastes (cotton seed cover and groundnut shell). The adsorbents were characterized and then applied as adsorbent for the fluoride removal from water. The adsorbent demonstrated good fluoride removal efficiency at the optimum conditions. The optimum reaction conditions were 180 min for reaction time, pH 5, 4 g/L adsorbent load and 323 K temperature. The fluoride removal efficiencies at the optimum conditions was 89 % and 90% for CNF and GNF, respectively which shows that the adsorption capacity for fluoride ions by these adsorbents was good. Further investigation about reusability was also done by washing the adsorbents with distilled water and reusing it up to five cycles to remove fluoride. The adsorbents' performance was almost at the 5th adsorption run demonstrating the high capacity for reusability. These adsorbents have hence, proved to be efficient, stable and reusable towards adsorption reactions. This work provides a novel finding on the use of environmental friendly, low cost and biodegradable materials for the treatment of water related issues.

ACKNOWLEDGEMENTS

The authors are thankful to Seed Grant (MU/R&D/21-22/MRP/FS05) for financial support from Marwadi University, Rajkot, Gujarat, India.

CONFLICT OF INTEREST

The authors declare that there is no conflict of interests regarding the publication of this article.

REFERENCES

1. H. Du, W. Liu, M. Zhang, C. Si, X. Zhang and B. Li, *Carbohydr. Polym.*, **209**, 130 (2019); https://doi.org/10.1016/j.carbpol.2019.01.020
2. M. El Achaby, N. El Miri, A. Aboulkas, M. Zahouily, E. Bilal, A. Barakat and A. Solhy, *Int. J. Biol. Macromol.*, **96**, 340 (2017); https://doi.org/10.1016/j.ijbiomac.2016.12.040
3. J.C. Bastidas, R. Venditti, J. Pawlak, R. Gilbert, S. Zauscher and J. Kadla, *Carbohydr. Polym.*, **62**, 369 (2005); https://doi.org/10.1016/j.carbpol.2005.08.058
4. J.I. Morán, V.A. Alvarez, V.P. Cyras and A. Vázquez, *Cellulose*, **15**, 149 (2008); https://doi.org/10.1007/s10570-007-9145-9
5. L. Jasmania and W. Thielemans, *Nanomedicine*, **4**, 14 (2018); https://doi.org/10.17352/2455-3492.000026
6. R. Rani, A. Singh and W. Ahmad, *Int. J. Health Clin. Res.*, **2**, 1 (2019).
7. N.A. Abdullah, M.S.A. Rani, M. Mohammad, M.H. Sainorudin, N. Asim, Z. Yaakob, H. Razali and Z. Emdadi, *Polimery*, **66**, 155 (2021); https://doi.org/10.14314/pol i mer y.2021. 3.1
8. S. Collazo-Bigliardi, R. Ortega-Toro and A. Chiralt Boix, *Carbohydr. Polym.*, **191**, 205 (2018); https://doi.org/10.1016/j.carbpol.2018.03.022
9. S. Mateo, S. Peinado, F. Morillas-Gutiérrez, M.D. La Rubia and A.J. Moya, *Processes*, **9**, 1594 (2021); https://doi.org/10.3390/pr9091594
10. J.M. Yarbrough, M.E. Himmel and S.Y. Ding, *Biotechnol. Biofuels*, **2**, 17 (2009); https://doi.org/10.1186/1754-6834-2-17

11. R.J. Moon, A. Martini, J. Nairn, J. Simonsen and J. Youngblood, *Chem. Soc. Rev.*, **40**, 3941 (2011); https://doi.org/10.1039/c0cs00108b
12. L. Brinchi, F. Cotana, E. Fortunati and J.M. Kenny, *Carbohydr. Polym.*, **94**, 154 (2013); https://doi.org/10.1016/j.carbpol.2013.01.033
13. T. Theivasanthi, F.L. Anne Christma, A.J. Toyin, S.C.B. Gopinath and R. Ravichandran, *Int. J. Biol. Macromol.*, **109**, 832 (2018); https://doi.org/10.1016/j.ijbiomac.2017.11.054
14. S. Eyley and W. Thielemans, *Nanoscale*, **6**, 7764 (2014); https://doi.org/10.1039/C4NR01756K
15. D. Trache, M.H. Hussin, M.K.M. Haafiz and V.K. Thakur, *Nanoscale*, **9**, 1763 (2017); https://doi.org/10.1039/C6NR09494E
16. K. Harini and C. Chandra Mohan, *Int. J. Biol. Macromol.*, **163**, 1375 (2020); https://doi.org/10.1016/j.ijbiomac.2020.07.239
17. Z. Kassab, M. El Achaby, Y. Tamraoui, H. Sehaqui, R. Bouhfid and A.E.K. Qaiss, *Int. J. Biol. Macromol.*, **136**, 241 (2019); https://doi.org/10.1016/j.ijbiomac.2019.06.049
18. M. Fazeli, M. Keley and E. Biazar, *Int. J. Biol. Macromol.*, **116**, 272 (2018); https://doi.org/10.1016/j.ijbiomac.2018.04.186
19. A. Dufresne, *Curr. Opin. Colloid Interface Sci.*, **29**, 1 (2017); https://doi.org/10.1016/j.cocis.2017.01.004
20. V. Nang An, H.T. Chi Nhan, T.D. Tap, T.T.T. Van, P. Van Viet and L. Van Hieu, *J. Polym. Environ.*, **28**, 1465 (2020); https://doi.org/10.1007/s10924-020-01695-x
21. A.G. Souza, D.F. Santos, R.R. Ferreira, V.Z. Pinto and D.S. Rosa, *Int. J. Biol. Macromol.*, **165**, 1803 (2020); https://doi.org/10.1016/j.ijbiomac.2020.10.036
22. R.M. Santos, W.P. Flauzino Neto, H.A. Silvério, D.F. Martins, N.O. Dantas and D. Pasquini, *Ind. Crops Prod.*, **50**, 707 (2013); https://doi.org/10.1016/j.indcrop.2013.08.049
23. W.P.F. Neto, H.A. Silvério, N.O. Dantas and D. Pasquini, *Ind. Crops Prod.*, **42**, 480 (2013); https://doi.org/10.1016/j.indcrop.2012.06.041
24. F. Rafieian, M. Shahedi, J. Keramat and J. Simonsen, *Ind. Crops Prod.*, **53**, 282 (2014); https://doi.org/10.1016/j.indcrop.2013.12.016
25. C.S. Lee, J. Robinson and M.F. Chong, *Process Saf. Environ. Prot.*, **92**, 489 (2014); https://doi.org/10.1016/j.psep.2014.04.010
26. J. Blockx, A. Verfaillie, O. Deschaume, C. Bartic, K. Muylaert and W. Thielemans, *Nanoscale Adv.*, **3**, 4133 (2021); https://doi.org/10.1039/D1NA00102G
27. S.V. Mayani, S.P. Bhatt, D.S. Padariya and V.J. Mayani, *Water Air Soil Pollut.*, **234**, 466 (2023); https://doi.org/10.1007/s11270-023-06482-7
28. M. Hashemkhani, M.R. Ghalhari, P. Bashardoust, S.S. Hosseini, A. Mesdaghinia and A.H. Mahvi, *Sci. Rep.*, **12**, 9655 (2022); https://doi.org/10.1038/s41598-022-13756-3
29. E.H. Qua, P.R. Hornsby, H.S.S. Sharma and G. Lyons, *J. Mater. Sci.*, **46**, 6029 (2011); https://doi.org/10.1007/s10853-011-5565-x
30. S. Lu, T. Ma, X. Hu, J. Zhao, X. Liao, Y. Song and X. Hu, *J. Sci. Food Agric.*, **102**, 312 (2022); https://doi.org/10.1002/jsfa.11360
31. W. Li, R. Wang and S. Liu, *BioRes.*, **6**, 4271 (2011); https://doi.org/10.15376/biores.6.4.4271-4281
32. A. Bhatnagar and M. Sain, *J. Reinf. Plast. Compos.*, **24**, 1259 (2005); https://doi.org/10.1177/0731684405049864
33. R. Li, J. Fei, Y. Cai, Y. Li, J. Feng and J. Yao, *Carbohydr. Polym.*, **76**, 94 (2009); https://doi.org/10.1016/j.carbpol.2008.09.034
34. B.O. Hong, F. Chen and G. Xue, *Cellulose Chem. Technol.*, **50**, 225 (2016).
35. A.S. Amarasekara, B. Wiredu and Y.M. Lawrence, *Carbohydr. Res.*, **475**, 34 (2019); https://doi.org/10.1016/j.carres.2019.02.002
36. M. Roman and W.T. Winter, *Biomacromolecules*, **5**, 1671 (2004); https://doi.org/10.1021/bm034519+
37. E.U.P. Barragán, C.F.C. Guerrero, A.M. Zamudio, A.B.M. Cepeda, T. Heinze and A. Koschella, *Fibers Polym.*, **20**, 1136 (2019); https://doi.org/10.1007/s12221-019-8973-1
38. C. Wu, D.J. McClements, M. He, L. Zheng, T. Tian, F. Teng and Y. Li, *Carbohydr. Polym.*, **255**, 117364 (2021); https://doi.org/10.1016/j.carbpol.2020.117364
39. B. Deepa, E. Abraham, N. Cordeiro, M. Mozetic, A.P. Mathew, K. Oksman, M. Faria, S. Thomas and L.A. Pothan, *Cellulose*, **22**, 1075 (2015); https://doi.org/10.1007/s10570-015-0554-x
40. A. Sonia and K. Priya Dasan, *Carbohydr. Polym.*, **92**, 668 (2013); https://doi.org/10.1016/j.carbpol.2012.09.015
41. Z.Z. Chowdhury and S.B.A. Hamid, *BioRes.*, **11**, 3397 (2016); https://doi.org/10.15376/biores.11.2.3397-3415
42. V.K. Gupta, I. Ali, T.A. Saleh, A. Nayak and S. Agarwal, *RSC Adv.*, **2**, 6380 (2012); https://doi.org/10.1039/C2RA20340E
43. M.S. Onyango, Y. Kojima, O. Aoyi, E.C. Bernardo and H. Matsuda, *J. Colloid Interface Sci.*, **279**, 341 (2004); https://doi.org/10.1016/j.jcis.2004.06.038
44. Y. Zhou, S. Fu, L. Zhang, H. Zhan and M.V. Levit, *Carbohydr. Polym.*, **101**, 75 (2014); https://doi.org/10.1016/j.carbpol.2013.08.055
45. R. Singh, S.P. Raghuvanshi and C. Kaushik, *Asian J. Chem.*, **20**, 5818 (2008).
46. D.J. Killedar and D.S. Bhargava, *Indian J. Environ. Health*, **35**, 81 (1993).